Self-Assembled Metallic Nanowires on a Dielectric Support: Pd on Rutile TiO2(110)

ARTICLE *in* NANO LETTERS · JANUARY 2009

Impact Factor: 13.59 · DOI: 10.1021/nl802703e · Source: PubMed

NANO LETTERS

2009
Vol. 9, No. 1
155-159

Self-Assembled Metallic Nanowires on a Dielectric Support: Pd on Rutile TiO_2(110)

David S. Humphrey,[†] Gregory Cabailh,[†] Chi L. Pang,[†] Chris A. Muryn,[‡] Stuart A. Cavill,[§] Helder Marchetto,[§,||] Alessandro Potenza,[§] Sarnjeet S. Dhesi,[§] and Geoff Thornton*[,†]

London Centre for Nanotechnology and Department of Chemistry, University College London, London WC1H 0AJ, United Kingdom, School of Chemistry, University of Manchester, Manchester M13 9PL, United Kingdom, Diamond Light Source Ltd, Harwell Science and Innovation Campus, Didcot, Oxfordshire OX11 0DE, United Kingdom, and Fritz Haber Institute of the Max Planck Society, 14195 Berlin, Germany

Received September 5, 2008; Revised Manuscript Received November 25, 2008

ABSTRACT

Palladium nanoparticles supported on rutile TiO_2(110)-1 × 1 have been studied using the complementary techniques of scanning tunneling microscopy and X-ray photoemission electron microscopy. Two distinct types of palladium nanoparticles are observed, namely long nanowires up to 1000 nm long, and smaller dotlike features with diameters ranging from 80−160 nm. X-ray photoemission electron microscopy reveals that the nanoparticles are composed of metallic palladium, separated by the bare TiO_2(110) surface.

Directed self-assembling nanostructures offer considerable potential for nanoscale electronics. A crucial component of these electronic devices will be quasi-1D wires supported on a dielectric support.[1−7] The inclusion of a wide band gap support is key as this ensures that conducting nanostructures are electrically isolated from the substrate. TiO_2-supported metal nanoparticles have been studied extensively due to wide-ranging applications in a number of technologies.[8,9] For instance, Pd/TiO_2 has been employed as a model catalyst system.[10−12] The TiO_2(110)-1 × 1 surface has an anisotropic surface structure,[13] which is of particular interest as such substrates allow the directed growth of nanostructures.[5−7]

In this study, we have used the structurally sensitive technique of scanning tunneling microscopy (STM) and chemically sensitive spectro-microscopy[14] to investigate the growth of metallic nanowires supported on a model dielectric substrate, namely Pd on TiO_2(110)-1 × 1. The Pd nanowires are grown by metal vapor deposition of Pd onto the TiO_2(110) surface held at elevated temperature. This enables rapid diffusion of Pd, facilitating growth of wires 5 nm wide and up to 1 μm in length with the [001] orientation determined by the anisotropy of the TiO_2(110)-1 × 1 surface.

Measurements employed two instruments. One is an Omicron variable temperature STM in London, operated at room temperature with a base pressure of $\sim 1 \times 10^{-10}$ mbar. All STM images were recorded using a W tip with positive sample bias in the constant current mode. X-ray photoemission electron microscopy (XPEEM) and low energy electron microscopy (LEEM) measurements were carried out at the Diamond Light Source, using the I06-Nanoscience soft X-ray beamline.[15] The end-station is an Elmitec LEEM III spectroscopic photoemission and low energy electron microscope (SPELEEM). In this instrument, photoemission and X-ray absorption measurements can currently be performed at a spatial resolution of about 50 nm with a typical photon energy (hυ) resolution of ~70 meV at 450 eV, and an energy resolution of ~300 meV of the electron analyzer during XPEEM imaging.

Rutile TiO_2(110) samples (Pi-Kem) were prepared with cycles of Ar^+ sputtering and annealing to 1000 K until a sharp 1 × 1 LEED pattern was obtained with no detectable contaminants in Auger electron spectroscopy or photoemission. Pd was dosed in situ by metal vapor deposition from a Pd wire (Advent and Goodfellow, 99.95%) onto a TiO_2(110) substrate held at 900 K.

* To whom correspondence should be addressed. E-mail: g.thornton@ucl.ac.uk. Telephone: +44-(0)207-679-7979. Fax: +44-(0)207-679-0595.
[†] University College London.
[‡] University of Manchester.
[§] Diamond Light Source Ltd.
[||] Fritz Haber Institute of the Max Planck Society, 14195 Berlin, Germany.

10.1021/nl802703e CCC: $40.75
Published on Web 12/29/2008

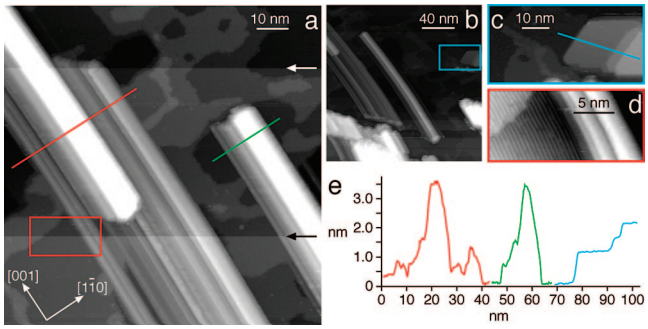

Figure 1. STM images of TiO_2(110) after depositing Pd at 900 K. Images recorded at constant current (1.08 V, 0.5 nA). (a) 100 × 100 nm^2. (b) 200 × 200 nm^2. Pseudohexagonal islands (blue box, expanded in (c) (~55 × 27 nm^2)) are observed in addition to nanowire structures. The red box in panel (a) highlights the area of image (d) (~20 × 9 nm^2) in which atomic Ti rows can still be imaged. Arrows indicate tip changes during scanning. Line profiles measured over the nanoparticles are shown (e).

Figure 1 shows STM images of Pd nanostructures on TiO_2(110)-1 × 1. In Figure 1a, there are two nanowires separated by ~15 nm. Figure 1b contains two types of nanostructures: nanowires and large pseudohexagonal islands. The image of the latter is expanded in Figure 1c. Between these nanostructures, the TiO_2 substrate can be seen with clear terraces and steps. Furthermore, in high resolution images, such as in Figure 1d, atomic scale rows with a periodicity of 0.65 nm can clearly be seen running in the [001] direction. These rows are characteristic of the TiO_2(110)-1 × 1 surface[13] and indicate that the nanowires align in the [001] direction. The isolated nanowire in the center of Figure 1b is ~170 nm long and ~4 nm high, while the flat top of the nanowire on the left of Figure 1b indicates a width of about 5 nm. The apparent uniform profile of the differing nanowires results from a convolution of the surface features with the tip morphology.

A second type of Pd nanostructure is also observed that consists of flat-topped pseudohexagonal islands, similar to those previously observed on TiO_2(110)-1 × 2.[9] In Figure 1c, an island ~30−50 nm wide can be seen containing three steps. The first step from the substrate is 1.04 ± 0.03 nm high, and subsequent steps are 0.46 ± 0.03 nm high. The 0.46 nm steps are twice the height of the Pd(111) interplanar spacing of 0.22 nm,[9] indicative of double atomic steps. The first step is about four atomic Pd spacings.

Although our STM images provide detailed information concerning the morphology of these nanostructures, they do not provide any chemical information. For this we turn to spectro-microscopy[14] to provide a chemical analysis of the nanostructures on a particle-by-particle basis. This prevents nanowire contributions being convoluted with those from the pseudohexagonal islands. On the I06-Nanoscience beamline, initial characterization employed LEEM (images not shown), which confirm the presence of both nanowires and islands. The apparent width of the islands varied between ~80−160 nm. Nanowires have a consistent apparent width of 120 ± 20 nm, and extend up to ~1 μm in length. The apparent width of features will be dominated by instrumental broadening including that arising from local field distortions. The actual width of features is expected to be in line with that observed with STM.

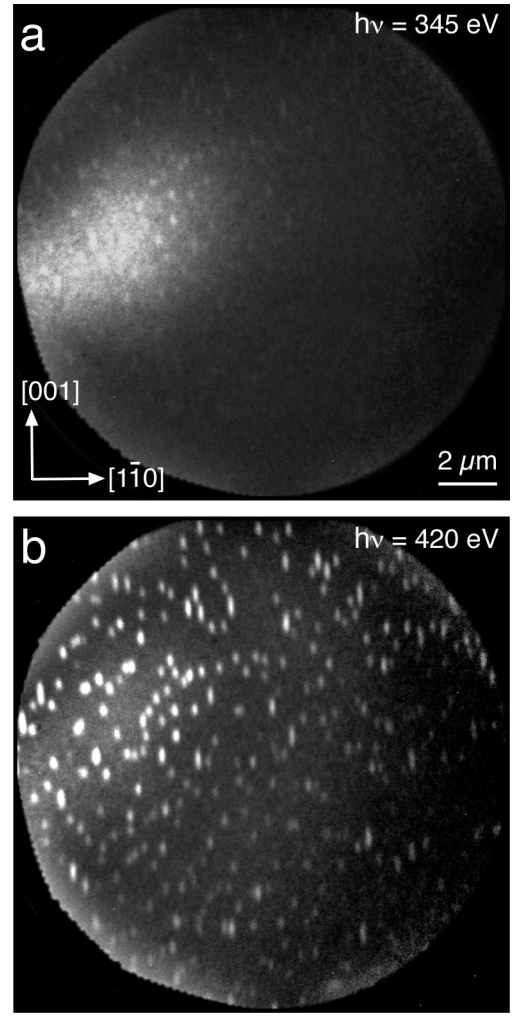

Figure 2. XPEEM secondary electron images of TiO_2(110) after depositing 1.4 ML Pd at 900 K. Images recorded with a 20 μm field of view. The photon energy is 345 eV (a) and 420 eV (b), below and above the Pd $M_{4,5}$ edge, respectively.

Figure 2 shows two secondary electron X-ray photoemission electron microscopy (XPEEM) images of Pd nanoparticles with a 20 μm field of view. In this XPEEM mode, secondary electrons with a kinetic energy of 0−5 eV are collected. In Figure 2a, the photon energy is set at 345 eV, which is just below the Pd $M_{4,5}$ edge (349 eV[16]), so that little intensity is observed directly from the Pd structures. In Figure 2b, the photon energy is set at 420 eV, above the Pd absorption edge, and Pd-related features become visible. This confirms that the bright features in Figure 2b correspond to Pd structures. An image with a 10 μm field of view is shown in Figure 3, where the morphology of the two types of nanoparticles is clearly distinguished.

A second XPEEM mode exploits the chemical sensitivity of the technique even further. Here, images are recorded at a single photon energy, collecting emitted photoelectrons with a narrow energy dispersion (0.6 eV). This energy-filtered XPEEM mode allows the chemical state of individual nanostructures to be monitored through the chemical shift of photoemission features. By scanning the kinetic energy,

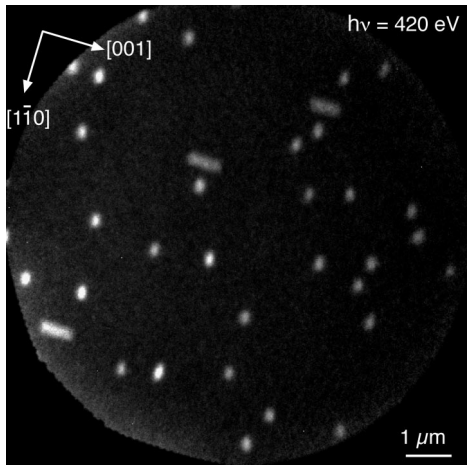

Figure 3. XPEEM secondary electron image of TiO_2(110) after depositing 0.4 ML Pd at 900 K. Image recorded with a 10 μm field of view. The photon energy is set at 420 eV so that Pd features are highlighted.

a sequence of images can be collected that is analogous to X-ray photoelectron spectroscopy (XPS), but which is also spatially resolved. In Figure 4a−d, four images are shown from a spectral-XPEEM movie recorded over the Pd $3d_{3/2}$ and $3d_{5/2}$ core levels (movie available online in Supporting Information). The kinetic energy of photoelectrons was scanned over 8 eV in 0.2 eV steps, corresponding to binding energies (E_B) of 342.1−334.1 eV. The four images displayed in Figure 4a−d are individual frames that demonstrate the essence of the XPS spectral information contained in the movie. Frame 4a is recorded at E_B = 342.1 eV, just above the Pd $3d_{3/2}$ core level. Frame 4b is located exactly on the Pd $3d_{3/2}$ core level at E_B = 340.1 eV. Frame 4c is recorded at E_B = 337.1 eV and lies between Pd $3d_{3/2}$ and $3d_{5/2}$. Finally, frame 4d is on the Pd $3d_{5/2}$ core level at E_B = 334.7 eV. Figure 4e is a secondary electron XPEEM image of the same area as the spectral-XPEEM movie and can be used as a map to identify individual nanoparticle positions in each of the movie frames.

Figure 4f shows three XPS spectra recorded using two different measurement modes. The first mode (red spectrum, Figure 4f) is performed by imaging the dispersive plane of the energy analyzer, sampling electrons from the entire field

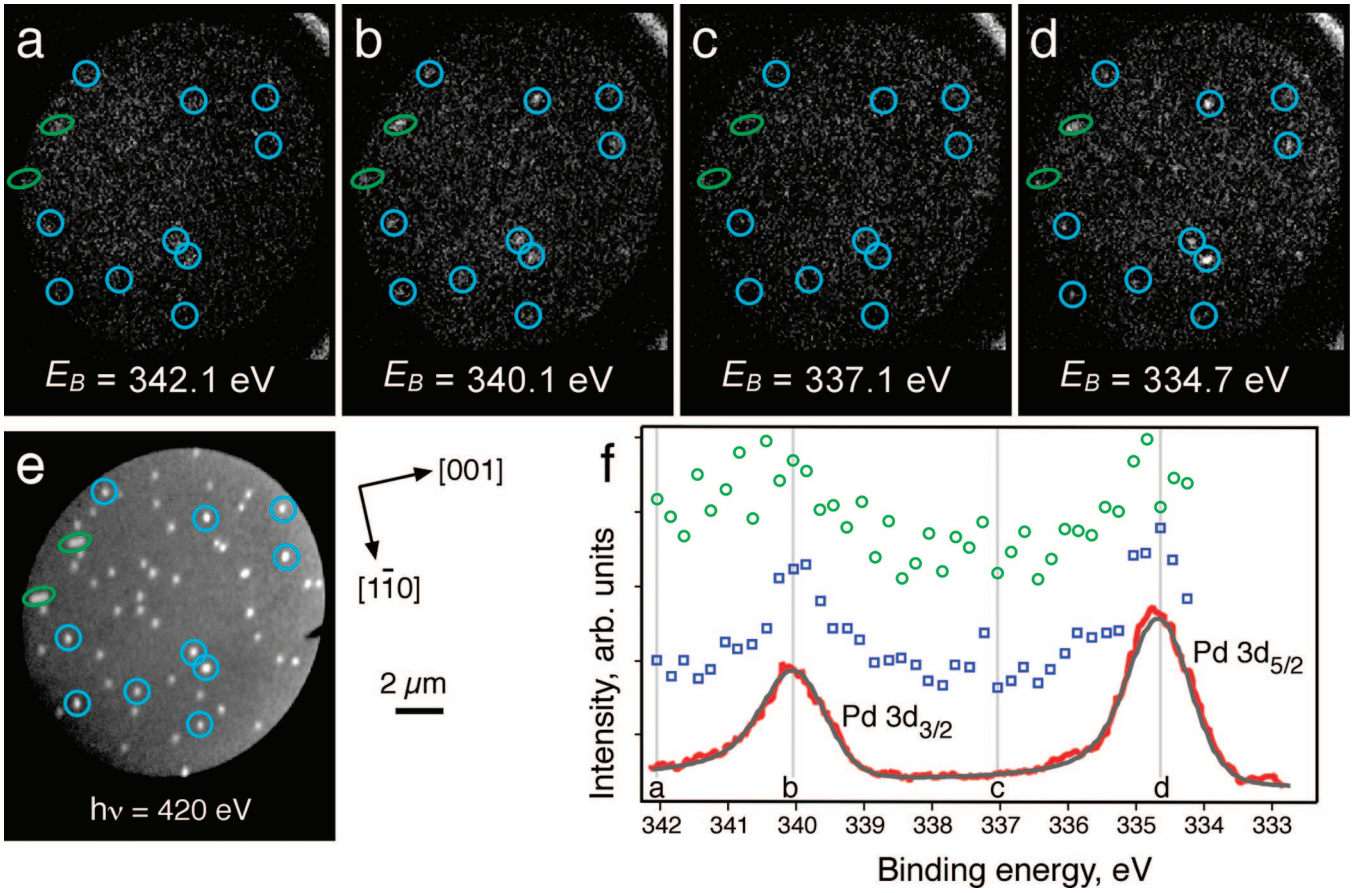

Figure 4. XPEEM images and XPS of TiO_2(110) after depositing 0.4 ML Pd at 900 K. XPEEM images recorded at ~13 μm field of view and 420 eV photon energy. Spectral-XPEEM images (a−d) correspond to binding energies of 342.1 eV (off core level), 340.1 eV (on core level), 337.1 eV (off core level), and 334.7 eV (on core level), respectively. Image (e) (corresponding to the same area as panels a−d) is an XPEEM secondary electron image recorded above the Pd $M_{4,5}$ edge at hν = 420 eV and shows all of the Pd-related features. In (f), the Pd 3d μXPS signal acquired at hν = 640 eV from a 20 μm field of view is displayed as a red curve (from a different region to the movie). The line shape was fitted using a Doniac−Sunjic function (gray line). Spectra from 10 Pd dotlike nanoparticles are displayed in blue and from 2 nanowires in green. Blue and green circled areas display the regions sampled to generate the nanoparticle and nanowire spectra, respectively. Light gray lines in the spectra correspond to the image energies of a−d. The oval shape of the field of view is created by a contrast aperture in the imaging optics.

of view, and is known as micro-XPS (μXPS) due to the micrometer-scale sampling areas used.[14,17] The second method (green and blue spectra, Figure 4f) is built up pixel-by-pixel from the spectral-XPEEM image sequence, selecting the sampling area over individual features.[14,17] The photon energy was selected to generate photoelectrons of ~70 eV KE which enhances the surface sensitivity of the measurements. The O 1s core level energy (530.0 eV) and the spin−orbit splitting of the Ti 2p core levels (5.8 eV), recorded at the same photon energy (640 eV), were used to extract the core level binding energies of the Pd 3d core levels. The Pd core level peak shape was fitted using an asymmetric Doniach−Sunjic line shape[18] and a Shirley background.[19] It was also necessary to use a polynomial correction for the background fitting, due to a difference in sensitivity across the detector (evaluated in spectra recorded from background regions).

The red curve in Figure 4f is a μXPS spectrum of the Pd 3d core levels recorded over the entire 20 μm field of view (sampled in a different area to the XPEEM movie), hence integrating signal from both the substrate and the nanoparticles. The Pd 3d core levels display asymmetry and Pd $3d_{5/2}$ was measured at a binding energy of 334.8 ± 0.5 eV, which corresponds to the lower end of values for metal Pd reported in the literature, 335.2 ± 0.4 eV.[20] The measured spin−orbit splitting of 5.3 ± 0.3 eV is also consistent with the literature values. The formation of a minority oxide component cannot be ruled out due to the presence of some signal intensity ~1.3 eV higher in binding energy from the main peaks.[20] A difference in the apparent width of the two main peaks can be attributed to Pd interband coexcitations that would give rise to features at 4 and 7 eV higher binding energies.[21−23]

The blue and green curves (Figure 4f) are averaged spectra recorded from the energy-filtered XPEEM movie, over 10 dotlike nanoparticles and 2 nanowires, respectively. The spectra are normalized using the substrate signal measured between nanoparticles as the background. The background contains no features corresponding to the Pd 3d core levels. The lower signal-to-noise compared to the μXPS spectrum (red) is due to the much smaller areas sampled. The total areas sampled for the dotlike structures and the nanowires are ~400 and ~2000 times smaller than for the red spectrum, respectively. The key result is that peaks for the nanoparticles correspond to those of the μXPS spectrum, the latter being consistent with metallic Pd. Recent high resolution XPS and X-ray absorption near-edge spectroscopy data from a similarly prepared Pd/TiO_2(110) sample[24] indicate that there is no TiO_x encapsulation of the nanoparticles.

Pd deposited onto TiO_2(110) surfaces at room temperature grows preferentially at step edges, except on highly defective surfaces where Pd is distributed across terraces.[25] This defect mediated growth is predicted by density functional theory calculations which show that a strong bond is formed when Pd adsorbs at oxygen vacancies.[26] The substrate anisotropy also plays a role in the particle distribution. Anisotropic diffusion on the TiO_2(110) surface is known to lead to strong spatial correlations for supported metals.[27,28] This is reflected in autocorrelation analyses that reveal a strong anticorrelation in the [001] direction, consistent with faster diffusion along rows compared with across rows.[27,28] An autocorrelation analysis of our nanoparticles also shows this strong anticorrelation along the [001] rows.

Deposition at higher temperature results in changes to the particle morphology. In previous work, Pd nanoparticles initially formed at 703 K and subsequently annealed to 723 K were shown to be elongated in the [001] direction with a maximum length of ~25 nm and width ~4 nm.[29] The origin of this anisotropic growth as well as the greater aspect ratio obtained here will result in part from enhanced mobility in the [001] direction, as predicted by recent calculations.[26] A similarly increased mobility is thought to give rise to the formation of atomic scale Pd 1D nanowires on SnO_2(101).[5]

The second factor that will play a key, and possibly the dominating role is the small lattice mismatch of the lowest energy plane termination of Pd, Pd(111)//[$1\bar{2}1$] with TiO_2(110)// [001] (7.1%) compared to Pd(111)//[$10\bar{1}$] with TiO_2(110)// [$1\bar{1}0$] (26.7%). This elongation is observed for Pd structures grown on TiO_2(110)-1 × 1^{30} and 1 × 2 surfaces,[9,29] and for Pt on TiO_2(110)-1 × 1 surfaces.[31] However, the length of the Pd nanowires we observe is unparalleled.

In summary, two coexisting types of supported nanostructures were prepared on TiO_2(110)-1 × 1: elongated nanowires and pseudohexagonal islands. Crucially, XPEEM movies were employed to measure XPS from individual nanoparticles, revealing both types of nanostructure to be composed of metallic Pd. As such, for the first time, we have identified a route to grow metallic nanowires on a dielectric platform.

Acknowledgment. The authors thank Professor John A. Venables for valuable discussions. Financial support for this work was provided by the EPSRC, U.K. (Grant EP/C54188X/1).

Supporting Information Available: The spectral-XPEEM image sequence movie as outlined in Figure 4. This material is available free of charge via the Internet at http://pubs.acs.org.

References

(1) Campbell, C. T. *Surf. Sci. Rep.* **1997**, *27*, 1.
(2) Henry, C. R. *Surf. Sci. Rep.* **1998**, *31*, 235.
(3) Silly, F.; Castell, M. R. *Phys. Rev. Lett.* **2005**, *94*, 046103.
(4) Silly, F.; Powell, A. C.; Martin, M. G.; Castell, M. R. *Phys. Rev. B* **2005**, *72*, 165403.
(5) Katsiev, K.; Batzill, M.; Diebold, U.; Urban, A.; Meyer, B. *Phys. Rev. Lett.* **2007**, *98*, 186102.
(6) He, Z.; Smith, D. J.; Bennett, P. A. *Phys. Rev. Lett.* **2004**, *93*, 256102.
(7) Liu, B. Z.; Nogami, J. *Nanotechnology* **2003**, *14*, 873.
(8) Diebold, U. *Surf. Sci. Rep.* **2003**, *48*, 53.
(9) Bennett, R. A.; Pang, C. L.; Perkins, N.; Smith, R. D.; Morrall, P.; Kvon, R. I.; Bowker, M. *J. Phys. Chem. B* **2002**, *106*, 4688.
(10) Macleod, N.; Cropley, R.; Lambert, R. M. *Catal. Lett.* **2003**, *86*, 69.
(11) Gao, W.; Chen, J.; Guan, X.; Jin, R.; Zhang, F.; Guan, N. *Catal. Today* **2004**, *93−95*, 333.
(12) Kim, W. J.; Kang, J. H.; Ahn, I. Y.; Moon, S. H. *J. Catal.* **2004**, *226*, 226.
(13) Bikondoa, O.; Pang, C. L.; Ithnin, R.; Muryn, C. A.; Onishi, H.; Thornton, G. *Nat. Mater.* **2006**, *5*, 189.
(14) Locatelli, A.; Bauer, E. *J. Phys.: Condens. Matter* **2008**, *20*, 093002.
(15) Diamond Light Source Ltd., Beamline I06: Nanoscience web area. http://www.diamond.ac.uk/Beamlines/Beamlineplan/I06/index.htm (accessed November 30, 2007).

(16) Yeh, J. J.; Lindau, I. *At. Data Nucl. Data Tables* **1985**, *32*, 1.
(17) Locatelli, A.; Aballe, L.; Mentes, T. O.; Kiskinova, M.; Bauer, E. *Surf. Interface Anal.* **2006**, *38*, 1554.
(18) Doniach, S.; Sunjic, M. *J. Phys. C* **1970**, *3*, 285.
(19) Shirley, D. A. *Phys. Rev. B* **1972**, *5*, 4709.
(20) NIST X-ray Photoelectron Spectroscopy Database; NIST Standard Reference Database 20, Version 3.4 (Web Version). http://srdata.nist.gov/xps/ (accessed February 26, 2008).
(21) Chiarello, G.; Colavita, E.; De Crescenzi, M.; Nannarone, S. *Phys. Rev. B* **1984**, *29*, 4878.
(22) De Crescenzi, M.; Lozzi, L.; Picozzi, P.; Santucci, S. *Z. Phys. D* **1989**, *12*, 417.
(23) Mattogno, G.; Righini, G. *Surf. Interface Anal.* **1991**, *17*, 689.
(24) Humphrey, D. S.; Yim, C. M.; Muryn, C. A.; Shulte, K.; Zakharov, A.; Anderson, J. F.; Thornton, G. Unpublished work, 2008.
(25) Jak, M. J. J.; Konstapel, C.; van Kreuningen, A.; Chrost, J.; Verhoeven, J.; Frenken, J. W. M. *Surf. Sci.* **2001**, *474*, 28.
(26) Sanz, J. F.; Marquez, A. *J. Phys. Chem. C* **2007**, *111*, 3949.
(27) Jak, M. J. J.; Konstapel, C.; van Kreuningen, A.; Verhoeven, J.; Frenken, J. W. M. *Surf. Sci.* **2000**, *457*, 295.
(28) Zhou, J.; Chen, D. A. *Surf. Sci.* **2003**, *527*, 183.
(29) Bowker, M.; Smith, R. D.; Bennett, R. A. *Surf. Sci.* **2001**, *478*, L309.
(30) Suzuki, T.; Souda, R. *Surf. Sci.* **2000**, *448*, 33.
(31) Dulub, O.; Hebenstreit, W.; Diebold, U. *Phys. Rev. Lett.* **2000**, *84*, 3646.

NL802703E